7.B.1
8.A.8
Nuclear Physics B5 (1968) 411-430. North-Holland Publ. Comp.. Amsterdam

ASYMPTOTIC PROJECTIONS OF SCATTERING MODELS

V. BARGER, M. OLSSON and D. D. REEDER
Department of Physics, University of Wisconson.*
Madison, Wisconsin 53706

Received 11 March 1968

Abstract: In an effort to delineate predictions of current phenomenological scattering models that can be tested on higher-energy accelerators, we have extrapolated models for total cross sections, ratio of real to imaginary amplitudes at $t = 0$, and elastic scattering differential cross sections to the 50-1000 GeV/c momentum range. We find that the asymptotic limit is essentially reached by 200 GeV/c in Regge-pole models that have a Pomeranchuk trajectory. The predictions of a model with zero total cross sections at infinity are contrasted with a model having constant asymptotic total cross sections. Extrapolations of a conventional diffraction model are briefly considered.

1. INTRODUCTION

Within the next decade, the highest obtainable accelerator kinetic energy is expected to increase thirtyfold: USSR (70 GeV, 1968); USA (200 GeV, 1973); Europe (300 GeV, ?); CERN (1000 GeV pp colliding beams, 1972). In addition, cosmic-ray experiments in progress should provide data on total cross sections and elastic scattering in the 100-300 GeV range. Among the interesting questions that will be investigated at these higher energies is the question of asymptotic boundary conditions for scattering theories. Over the range of energies studied at the present, phenomenological models based on the idea of Regge-pole dominance have been reasonably successful in quantitatively describing the data. However, it is theoretically conceivable that Regge-pole dominance at higher energies may be appreciably modified by branch cuts in the complex angular momentum plane. An even more drastic possibility is that the Regge hypothesis may be inappropriate in the description of ultrahigh-energy phenomena and will be replaced by a different diffraction mechanism. In order to devise simple experimental tests of current Regge ideas that can be accomplished in the early experiments on the higher-energy accelerators, it is of interest to extrapolate to these higher energies

* Work supported in part by the University of Wisconsin Research Committee, with funds granted by the Wisconsin Alumni Research Foundation, and in part by the U. S. Atomic Energy Commission under contract AT(11-1)-881, COO-881-159.

Regge parametrizations which satisfactorily account for present data. Although it is widely recognized that these parametrizations are not unique, nevertheless, the extrapolations of the various models have qualitatively similar asymptotic features.

In this paper we concern ourselves with extrapolations to the TeV range of elastic-scattering and total cross section data using meson Regge-exchange models. In each case we consider extrapolations of several models so that the model-independent features can be adjudged. In the treatment of total cross sections in sect. 2, we have first refitted all the available data (including the recent BNL data [1] in the 8-28 GeV range) in terms of two representative Regge models; one has vanishing total cross sections at infinite energies, the other constant total cross sections. In the process of analyzing these data we discuss in passing a re-evaluation of symmetries for the meson-exchange vertices. For the elastic-scattering predictions of sect. 3, we have extrapolated the parametrizations of two current Regge models. Finally, as a representative diffraction scattering model, we consider extrapolations of the fit to the pp elastic-scattering data by Krisch [2]. Our goal here is simply to provide in easily accessible form projections into the TeV range which should be useful in the design of experiments. Undoubtedly some or even all of these projections may be disproved, but in being so disproved they will have served their purpose.

2. REGGE-POLE MODELS AND FORWARD ELASTIC SCATTERING

With the Regge-pole model it is possible to obtain a complete description of the present data on the total cross sections and the real part of the forward elastic amplitude. There are a number of simplifications [3] that occur in the analysis of meson-nucleon and nucleon-nucleon elastic scattering at the forward direction: (i) only helicity non-flip amplitudes are required, (ii) total cross sections are linearly related to the imaginary part of the amplitudes by the optical theorem, and (iii) only neutral, non-strange meson exchanges with $C = P = (-)^J$ can contribute to the spin-averaged forward amplitudes.

The spirit of the approach is to associate, as far as possible, the t-channel Regge poles with the observed meson states. Of the observed particles only the vector mesons (ρ^0, ω, ϕ) and the tensor mesons (A_2^0, f_0, f^*) need be considered as exchanges, according to the above quantum-number restrictions. An additional $I=0$ exchange (the Pomeranchuk) is also commonly allowed in the analyses, as discussed below. In table 1 two possible assignments of these trajectories to SU(3) multiplets of particles are listed. Symmetry principles are incorporated into the Regge model in a natural way by requiring the symmetry to apply to the factorized Regge residues [3].

For the odd-signature meson exchanges (ρ^0, ω, ϕ) we prefer not to impose a particular symmetry for the residues at the outset. Rather, we directly use the data to determine the residues and then compare the results with the symmetry predictions of SU(3) (refs. [3, 4]), universality [5], and

Table 1
The association of meson Regge trajectories with particles in two symmetry models.

Trajectory	Particle	SU(3) multiplet
P	p(1700)?	2^+ singlet
P'	f(1250)	
S	$f^*(1500)$ {decoupled from $\bar{N}N$	2^+ nonet
A	$A_2(1320)$	
ω	$\omega(783)$	
ϕ	$\phi(1020)$ {decoupled from $\bar{N}N$	1^- nonet
ρ	$\rho(750)$	
	Alternative assignment (only two $I=0$ 2^+ trajectories)	
P'	mixed { f(1250)	2^+ singlet
S	mixed { $f^*(1500)$	and octet
A	$A_2(1320)$	

the quark model *. Symmetry-breaking of the vector-meson trajectories is permitted in the analysis in that the trajectories are not constrained to be degenerate. The generality of our treatment of the vector-meson exchanges will be restricted by the assumption that the ϕ-meson exchange is decoupled from the $\bar{N}N$ vertex. There exists supporting theoretical and experimental evidence for the validity of this assumption [7]. Finally, the physical ω and ϕ particles are treated as the appropriate exchanges, with the mixing angle taken to be independent of momentum transfer [3].

The treatment of the even-signature meson exchanges will follow two proposed Regge models that show wide divergences in structure. A summary of the particle-trajectory associations in the two models is given in table 1. The two models to be analyzed in detail have been chosen not only because of their differing particle-trajectory assignments, but also because of their differing predictions in asymptotic extrapolations. In the more conventional model proposed by Barger and Olsson [3] the even-signature trajectories (A, P', S) are associated with the neutral, non-strange tensor mesons (A_2^0 f_0, f^*). The mixing between the two $I=0$ tensor trajectories is chosen to be the nonet mixing angle of the (f_0, f^*) particles, independent of momentum transfer. In analogy with the ϕ meson coupling, the S Regge pole is uncoupled from the $\bar{N}N$ vertex (a nonet coupling ansatz [7] which also follows from $\bar{q}_\Lambda q_\Lambda$ quark constituents for the f^* meson). In addition to these trajectories a unitary singlet Pomeranchuk trajectory with maximal intercept $\alpha_P(0)=1$ is introduced to give asymptotic constant cross sections.

* Ref. [6] contains many quark-model predictions for high-energy scattering as well as references to earlier work.

In the alternative theoretical model proposed by Cabbibo, Horwitz, Kokkedee and Ne'eman [8] (the CHKN model) there is no Pomeranchuk amplitude. Furthermore, an arbitrary mixing is allowed between the two isoscalar trajectories P' and S. The mixing angle is nearly zero at $t = 0$ due to the near asymptotic equality of πN and KN cross sections which requires that the leading trajectory be primarily a unitary singlet. The ratio of meson to nucleon couplings of the leading trajectory is constrained such that the asymptotic cross sections would be in the quark counting ratio $\sigma_{\pi N}/\sigma_{NN} = \frac{2}{3}$ in the limit of zero mixing - a limit not quite realized in the actual data analysis. In order to fit the experimental data the current-algebra constraint of pure F coupling is relaxed by allowing both F- and D-type tensor meson couplings to $\bar{N}N$. In the analysis both $\alpha_{P'}(0)$ and $\alpha_S(0)$ are determined to be significantly smaller than one, which means that total cross sections must vanish asymptotically.

Other variations of symmetry models for forward scattering have been suggested [9], but most embody the basic features of the above models. Since numerous models can more or less fit the present data, it is mainly of interest to categorize basically different types of solutions. In particular the discussion here will be limited to the two models mentioned above. In discussing the results of phenomenological fits to the data, we adopt the following notation for the forward amplitudes:

$$f(\bar{p}p) = \tfrac{3}{2}(P)_N + \tfrac{3}{2}(P')_N + \tfrac{1}{6}(A)_N + \tfrac{3}{2}(\omega)_N + \tfrac{1}{6}(\rho)_N ,$$

$$f(K^- p) = (P)_K + \tfrac{1}{2}(P')_K + \tfrac{1}{6}(A)_K + \tfrac{1}{2}(\omega)_K + \tfrac{1}{6}(\rho)_K ,$$

$$f(\pi^- p) = (P)_\pi + (P')_\pi + \tfrac{1}{3}(\rho)_\pi . \qquad (1)$$

The remaining scattering amplitudes are obtained by isospin and charge conjugation invariance. The numerical coefficients have been extracted so that the residues would be equal in appropriate symmetry limits (e.g., SU(3) (refs. [3, 4]), universality [5] and quark model [6]). Representative forms of the amplitudes are for even-signature exchange

$$(P)_K = \frac{1}{\sqrt{s}} \gamma_{P\bar{K}K} \gamma_{P\bar{N}N} (i - \cot \tfrac{1}{2}\pi\alpha_P) \left(\frac{E_{lab}}{E_0}\right)^{\alpha_P} , \qquad (2)$$

and for odd-signature exchange

$$(\omega)_K = \frac{1}{\sqrt{s}} \gamma_{\omega\bar{K}K} \gamma_{\omega\bar{N}N} (i + \operatorname{tg} \tfrac{1}{2}\pi\alpha_\omega) \left(\frac{E_{lab}}{E_0}\right)^{\alpha_\omega} . \qquad (3)$$

The scaling factor E_0 is chosen to be $E_0 = s_0/2M$ with $s_0 = 1(\mathrm{GeV})^2$. The optical theorem is $\sigma_t = (4\pi/q)\,\mathrm{Im}f$ where q is the c.m. momentum.

The experimental data on total cross sections in the 5 to 30 GeV/c momentum range are plotted in fig. 1. The $\pi^\pm$p and pp data are taken from the recent BNL experiment of Foley et al. [1]. Most of the other data come from the earlier BNL experiment of Galbraith et al. *. The large uncertainties in the $\bar{p}$n and pn data are evident.

* Ref. [10]. The cross sections σ_t(pp) and σ_t(pn) have also been measured at high energy by Bellettini et al. [11].

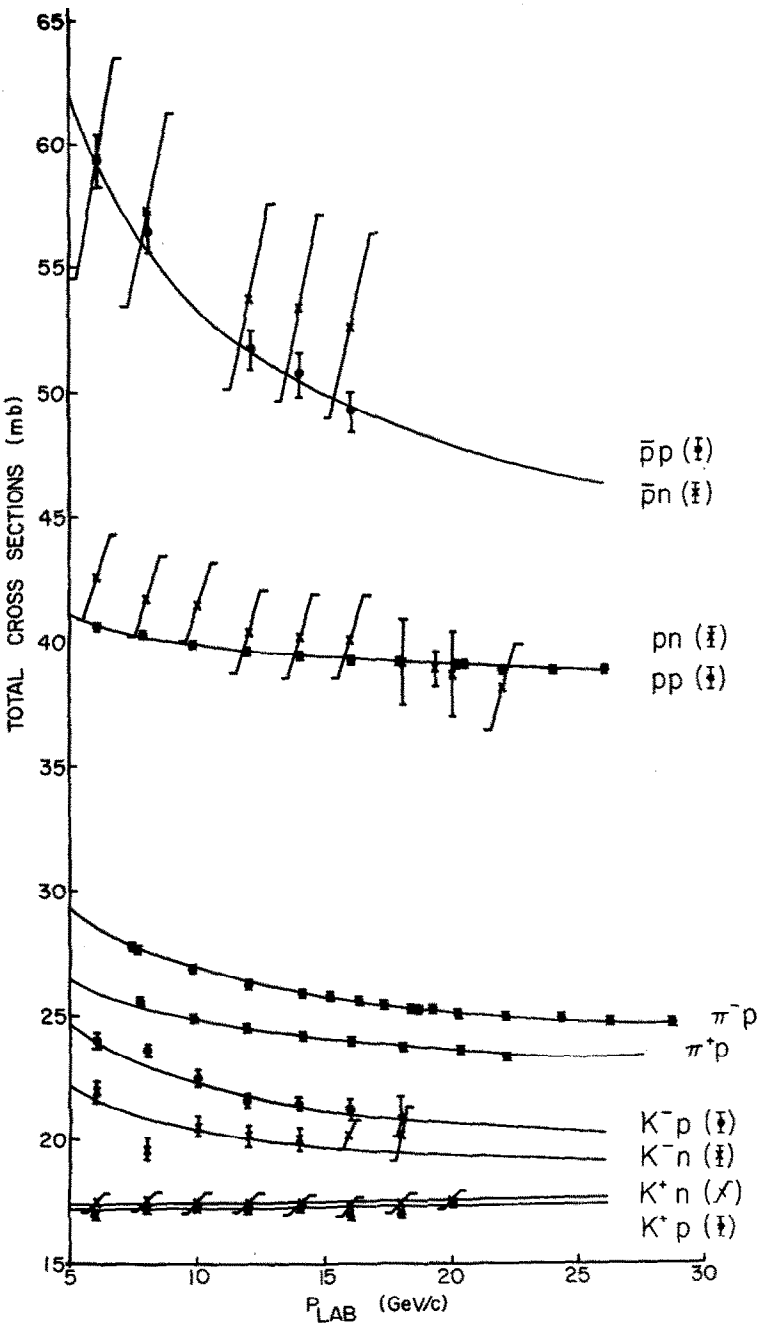

Fig. 1. Experimental measurements for total cross sections (refs. [1, 10]). The fitted curves represent the Barger-Olsson Regge pole symmetry model with (P, P', A, ω, ρ) trajectories. The curves for pp and pn coincide in this fit (likewise for $\bar{p}p$ and $\bar{p}n$).

Table 2
Regge parameters of the Barger-Olsson model determined from a fit to data on total cross sections, $(\mathrm{Re}f/\mathrm{Im}f)_{t=0}$ and forward charge-exchange data. For comparison, the predictions of various symmetry schemes for the Regge residues are indicated.

Fitted trajectory intercept	Regge residue	Fitted residue	SU(3)	ρ, ω universality	SU(3) quark model	(ρ, A) exchange degeneracy
$\alpha_P = 1$	$(P\pi\pi)(P\bar{N}N)$	2.16 ± 0.03	a		g	
	$(P\bar{K}K)(P\bar{N}N)$	1.77 ± 0.04	a		g	
	$(P\bar{N}N)^2$	2.45 ± 0.05			g	
$\alpha_{P'} = 0.51 \pm 0.03$	$(P'\pi\pi)(P'\bar{N}N)$	2.03 ± 0.08	b		h	
	$(P'\bar{K}K)(P'\bar{N}N)$	1.77 ± 0.31	b		h	
	$(P'\bar{N}N)^2$	3.02 ± 0.18			h	
$\alpha_A = 0.34 \pm 0.03$	$(A\pi\eta)(A\bar{N}N)$	1.6 ± 0.03	c		h	
	$(A\bar{K}K)(A\bar{N}N)$	1.7 ± 0.23	c		h	j
	$(A\bar{N}N)^2$	$0\ {}^{+1.7}_{-0}$			h	k
$\alpha_\omega = 0.38 \pm 0.04$	$(\omega\bar{K}K)(\omega\bar{N}N)$	2.5 ± 0.3		e	i	
	$(\omega\bar{N}N)^2$	2.8 ± 0.4		e	i	
$\alpha_\rho = 0.54 \pm 0.01$	$(\rho\pi\pi)(\rho\bar{N}N)$	1.1 ± 0.06	d	f	i	
	$(\rho\bar{K}K)(\rho\bar{N}N)$	1.2 ± 0.1	d	f	i	j
	$(\rho\bar{N}N)^2$	$0\ {}^{+0.9}_{-0}$		f	i	k

$\chi^2 = 122$
No. data = 165

repeated letter denotes predicted equality.
} denotes verification from fit.

The curves in fig. 1 represent the results of a simultaneous least-squares fit to the total cross section $(\mathrm{Re}f/\mathrm{Im}f)_{t=0}$ (ref. [1]) and forward charge exchange [12] data using the Barger-Olsson model with (P, P', A, ω, ρ) trajectories as previously described. The theoretical curves are in good agreement with the data. The A- and ρ-exchange residues in NN and $\bar{N}N$ scattering are essentially undetermined by the data and have been set to zero in this analysis (hence we obtain $\sigma_{pp} = \sigma_{pn}$ and $\sigma_{\bar{p}p} = \sigma_{\bar{p}n}$). The approximate constancy and equality of $\sigma_t(K^+p)$ and $\sigma_t(K^+n)$ arises from the approximate imaginary amplitude equalities

$$(P') \approx (\omega),$$

$$(A) \approx (\rho).$$

However, the corresponding residues and trajectories do not appear to be nearly so degenerate (c.f. table 2). In fig. 2 the corresponding theoretical curves for $(\mathrm{Re}f/\mathrm{Im}f)_{t=0}$ are compared with the recent data of Foley et al. [1]. The measurement errors on the data of Foley et al. [1] for the ratio of

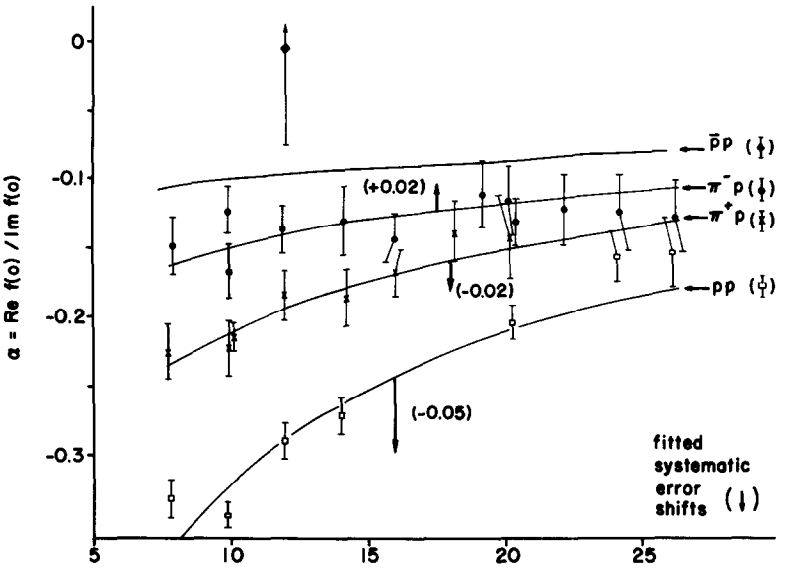

Fig. 2. Regge symmetry model fits to the experimental data of ref. [1] for the ratio of real to imaginary parts at $t=0$. The theoretical model incorporates (P, P', A, ω, ρ) exchanges.

real to imaginary amplitudes are divided into statistical and systematic parts. The experimental errors on $\alpha_{\pm} = (\mathrm{Re}f(\pi^{\pm}\mathrm{p})/\mathrm{Im}f(\pi^{\pm}\mathrm{p})_{t=0}$ are such that the systematic errors are expected to cancel when the sum $\alpha_+ + \alpha_-$ is formed. A normalization parameter was introduced in the fit for each type of real-part data and was varied as a parameter. As shown in fig. 2 these fitted normalization parameters have the expected cancellation in the combination $\alpha_+ + \alpha_-$.

The fitted parameters from this analysis are given in table 2. The results for the P', A and ρ residues are consistent within errors with the SU(3) predictions [3]. The A and ρ residues are primarily determined by the meson-nucleon charge exchange reactions and their symmetry properties have been discussed previously [4]. The Pomeranchuk couplings to $\pi\pi$ and $\bar{K}K$ differ by 20% from that expected of a unitary singlet *. The P' couplings to $\pi\pi$ and KK agree well with the SU(3) ratio *based on the mixing angle at the* $f^0(1250)$ *meson pole.* The χ^2 value of 122 indicates a good fit to the 165 data points.

The projection of Regge models to ultrahigh energies is of particular interest in the planning of early experiments to be made on the higher energy accelerators. In fig. 3 the total cross section projections of this (P, P', A, ω, ρ) model are shown for the 50 to 1000 GeV/c laboratory momentum range. By 200 GeV/c the total cross sections have leveled off and have essentially

* If the Pomeranchuk intercept is treated as a free parameter in the analysis, we find $\alpha_P(0) = 1.05 \pm 0.05$ which is in agreement with a "maximal" intercept of unity.

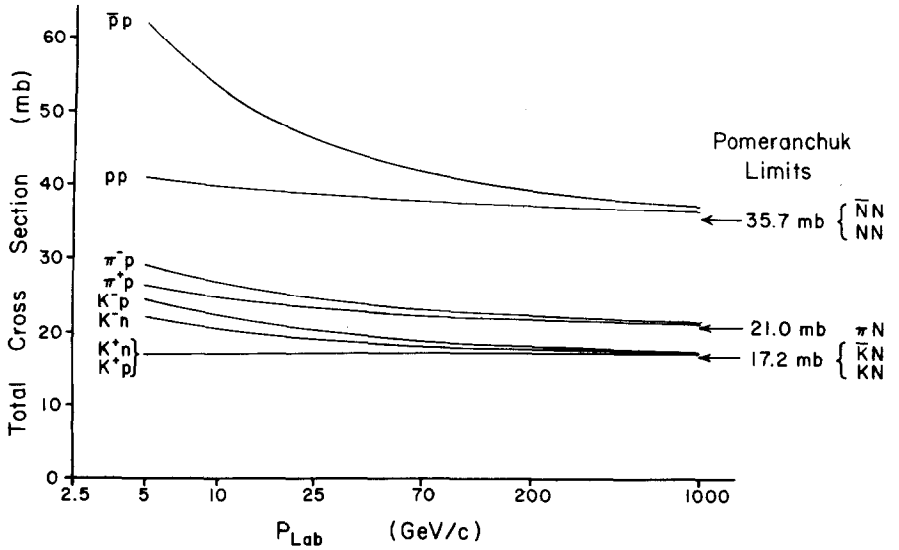

Fig. 3. Asymptotic projections of total cross sections from the (P, P', A, ω, ρ) Regge-symmetry model.

reached their respective Pomeranchuk limits. *If a Pomeranchuk trajectory exists, then total cross sections will remain fairly constant over the* 200-400 GeV/c *range. Furthermore, the symmetry breaking in the Pomeranchuk couplings to* $\pi\pi$ *and* $\bar{K}K$ *can be directly measured at these momenta.* The asymptotic projections of the Regge fit gave,

$$\frac{\sigma_t(NN)}{\sigma_t(KN)} \approx 2.1 \quad \text{and} \quad \frac{\sigma_t(NN)}{\sigma_t(\pi N)} \approx 1.7 .$$

The simple quark model [6] of scattering predicts 1.5 for these ratios.

The projections of $(\mathrm{Re}\, f/\mathrm{Im}\, f)_{t=0}$ to higher momenta are shown in fig. 4. Above 200 GeV/c all real parts are less than 10% of the corresponding imaginary parts.

The alternative model without a Pomeranchuk trajectory (i.e., no trajectory with $\alpha_P(0) = 1$) presents a completely different asymptotic picture with vanishing total cross sections at infinite energy. If ϕ is used to denote the mixing of the isoscalar tensor mesons, $\lambda = F - \frac{1}{3}D$, and $\gamma_{P'}$, γ_S denote the P' and S trajectory residues, the CHKN model [8] can be written in terms of the residues of eqs. (1) and (2) by the substitutions:

$$\gamma_{P\pi\pi}\gamma_{P\bar{N}N} = 2\gamma_{P'}(\sqrt{2}\cos\phi + \sin\phi)(\sqrt{2}\cos\phi + \lambda\sin\phi),$$

$$\gamma_{P\bar{K}K}\gamma_{P\bar{N}N} = \gamma_{P'}(2\sqrt{2}\cos\phi - \sin\phi)(\sqrt{2}\cos\phi + \lambda\sin\phi),$$

$$\gamma_{P\bar{N}N}^2 = 2\gamma_{P'}(\sqrt{2}\cos\phi + \lambda\sin\phi)^2,$$

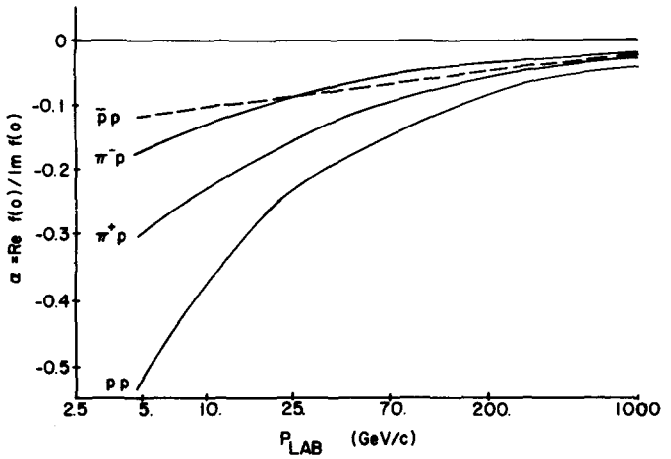

Fig. 4. Asymptotic projections of $\alpha = \{\mathrm{Re}f(0)/\mathrm{Im}f(0)\}$ from the (P, P', A, ω, ρ) Regge-symmetry model.

$$\gamma_{P'\pi\pi}\gamma_{P'\bar{N}N} = 2\gamma_S(\sqrt{2}\sin\phi - \cos\phi)(\sqrt{2}\sin\phi - \lambda\cos\phi),$$

$$\gamma_{P'\bar{K}K}\gamma_{P'\bar{N}N} = 2\gamma_S(2\sqrt{2}\sin\phi + \cos\phi)(\sqrt{2}\sin\phi - \lambda\cos\phi),$$

$$\gamma_{P'\bar{N}N}^2 = 2\gamma_S(\sqrt{2}\sin\phi - \lambda\cos\phi)^2.$$

The fits to the cross section and real parts data using the CHKN model are shown in figs. 5 and 6. (In this fit the ρ and ω parameters were constrained to have the values in table 2.) The residue and trajectory parameters are given in table 3. The χ^2 of 210 achieved in this fit is considerably higher than with the Pomeranchuk model; however this still does not rule out this general type of solution. Since no χ^2 minimum seemed to exist, we forced a solution close to that originally found by CHKN. The high energy projections of the total cross sections in this model are shown by the solid curves in fig. 7. The dashed curves are the projections of the fits from the Barger-Olsson model. The two solutions for σ_t(pp) differ by several millibarns by 200 GeV/c. Accurate σ_t(pp) and $\sigma_t(p\bar{p})$ data over the momentum range 25-70 GeV/c should differentiate the two solutions. Fig. 8 shows $(\mathrm{Re}f/\mathrm{Im}f)_{t=0}$ in the CHKN model. This ratio tends to the constant value

$$-\cot(\tfrac{1}{2}\pi\alpha_{P'}) \equiv -0.09,$$

asymptotically. In contrast $(\mathrm{Re}f/\mathrm{Im}f)_{t=0}$ approaches zero at high energy in the Barger-Olsson model.

3. ELASTIC SCATTERING PROJECTIONS

3.1. *Regge models*

The experimental data on elastic scattering above 3 GeV/c indicate vir-

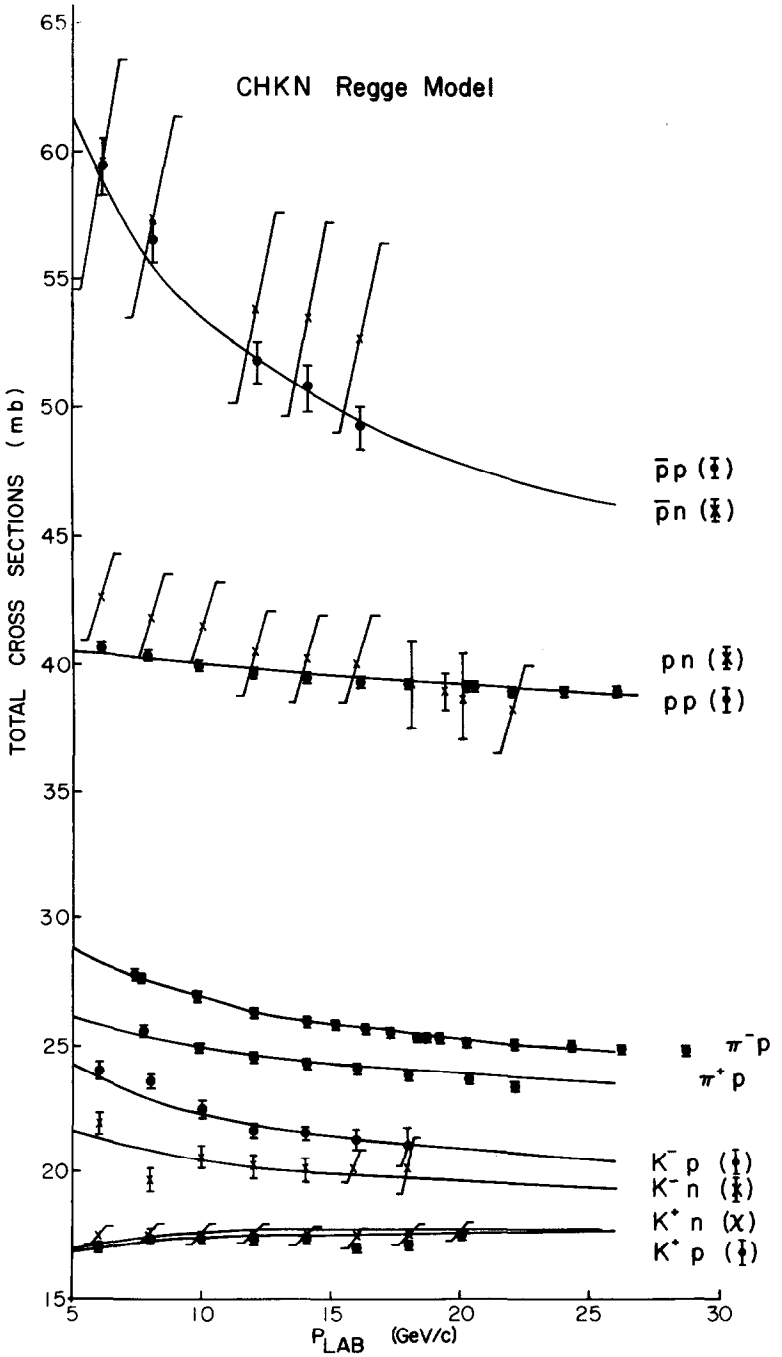

Fig. 5. Fits to total cross sections using the CHKN Regge model.

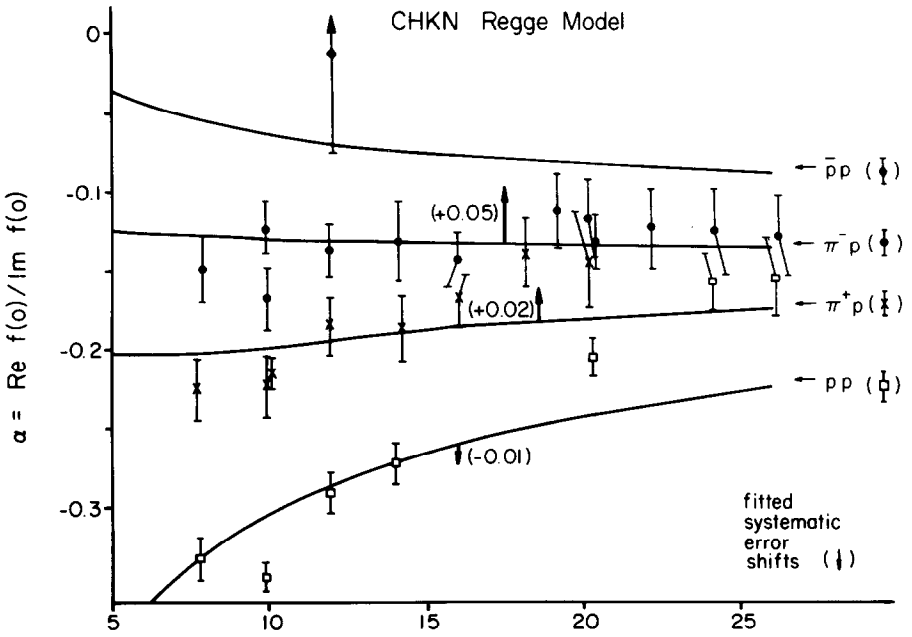

Fig. 6. Fits to $\alpha = \{\mathrm{Re}f(0)/\mathrm{Im}f(0)\}$ using the CHKN Regge model.

tually no isospin dependence *. For example, approximate equalities such as $d\sigma/dt(pp) \approx d\sigma/dt(pn)$ and $d\sigma/dt(\pi^- p) \approx d\sigma/dt(\pi^+ p)$ are experimentally observed. This fact is readily interpreted as evidence for the dominance of isoscalar meson exchanges. As discussed in sect. 2 these $I=0$ exchanges are usually chosen to be the P, P' and ω. The ω amplitude changes sign be-

Table 3
Regge parameters of the CHKN model determined from a fit to the data on total cross sections and $(\mathrm{Re}f/\mathrm{Im}f)_{t=0}$.

Trajectory	Residue
$\alpha_{P'} = 0.94 \pm 0.01$	$\gamma_{P'} = 0.58 \pm 0.02$
$\alpha_S = 0.68 \pm 0.1$	$\gamma_S = 0.17 \pm 0.02$
P', S mixing angle $\phi = 6^o \pm 2^o$	
F/D parameter $\lambda = F - \frac{1}{3}D = 2.19 \pm 0.02$	
$\chi^2 = 220.$ No. data = 165.	

* See for example ref. [13]; especially the reports by Barger, Longo and Perl review much of the existing experimental evidence for isospin independence.

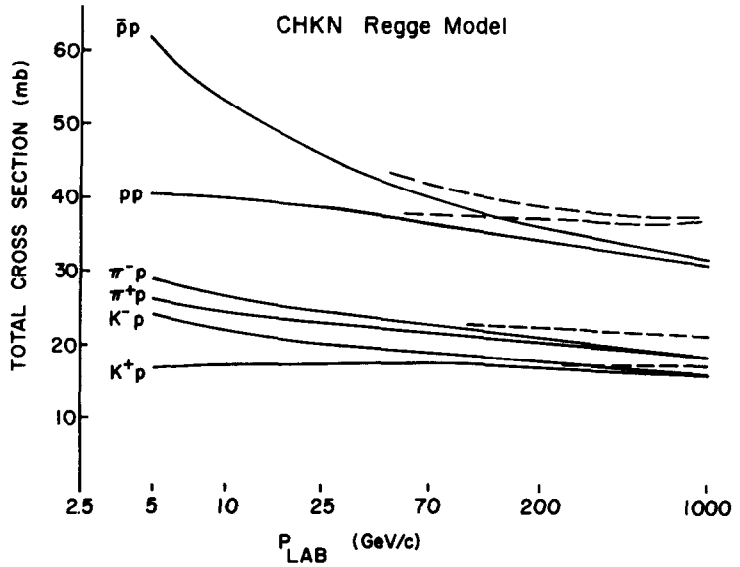

Fig. 7. Asymptotic projections of total cross sections from the CHKN Regge model. Dotted curves are results from fig. 3 of the Barger-Olsson model.

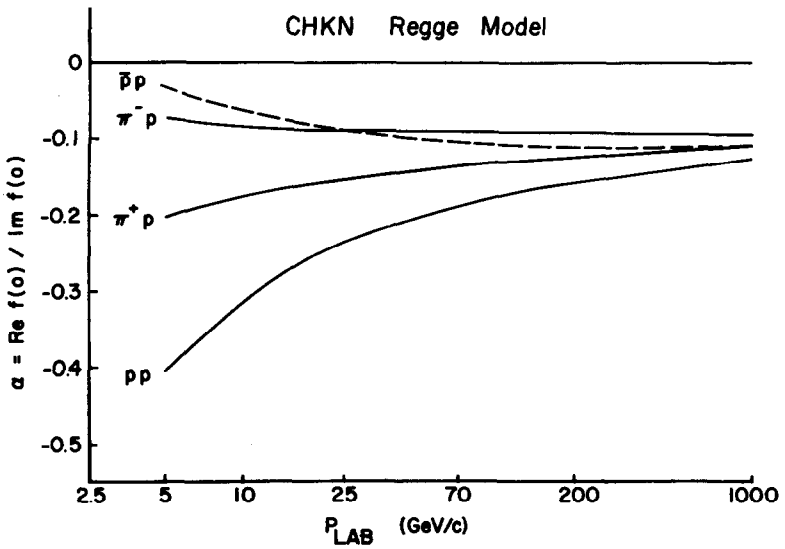

Fig. 8. Asymptotic projections of $\alpha = \{\mathrm{Re}f(0)/\mathrm{Im}f(0)\}$ from the CHKN Regge model.

tween NN and $\bar{N}N$ elastic amplitudes and thereby accounts for the marked differences in their angular distributions. The interference of ω with P + P' gives rise to the effective shrinkage in pp scattering and anti-shrinkage in $\bar{p}p$ scattering. The dominant t-channel helicity amplitudes for P and P' exchanges must be non-flip inasmuch as the elastic differential cross sections show no flattening near $t = 0$ as would result from large helicity flip amplitudes. The ω also has a sizeable helicity non-flip component. The relative magnitudes and characteristics of the helicity flip amplitudes of these three exchanges are not well established by present phenomenological analyses. Present polarization data do not adequately determine the flip amplitudes.

Finally, the non-shrinkage of the forward peaks in πN scattering requires a relatively flat Pomeranchuk trajectory. In particular its slope is constrained to be less than $\frac{1}{2}\,(\mathrm{GeV}/c)^{-2}$ with the smaller values preferred. In contrast the P' and ω trajectories are normally found to have the more conventional slopes of about $1\,(\mathrm{GeV}/c)^{-2}$.

Two representative parametrizations embodying the characteristics cited above have been proposed by Chiu, Chu and Wang [14] and by Rarita, Riddel, Chiu and Phillips [15] (here after referred to as CCW and RRCP respectively). A basic difference in the solutions obtained by these authors is the treatment of the isoscalar helicity flip amplitudes, arbitrarily set equal to zero by CCW (neglecting high energy pp polarization) but allowed to have significant magnitude by RRCP. In the projections presented below we consider solution 3 of RRCP and the solution obtained by CCW. Both solutions have a Pomeranchuk trajectory given approximately by

$$\alpha_{\mathrm{P}}(t) = 1 + \tfrac{1}{3}t.$$

In these Regge models the energy dependence will be governed by this trajectory at ultrahigh energies.

One of the most interesting projections from current Regge parametrizations concerns the effective shrinkage to be expected in the TeV energy range. In order to investigate this question we have used an effective one-pole trajectory approximation

$$\frac{\mathrm{d}\sigma}{\mathrm{d}t} = F(t)\left(\frac{E}{E_0}\right)^{2\alpha(t)-2},$$

to represent the multi-Regge pole situation. Using the above Regge models to calculate $\mathrm{d}\sigma/\mathrm{d}t$ we determine the effective trajectory at an energy E by the equation

$$2\alpha(t) - 2 = \frac{\ln\left[\frac{\mathrm{d}\sigma}{\mathrm{d}t}(E_+, t)\right] - \ln\left[\frac{\mathrm{d}\sigma}{\mathrm{d}t}(E_-, t)\right]}{\ln E_+ - \ln E_-},$$

where $E_\pm = E \pm \Delta E$ and ΔE is a small increment chosen to be $0.01\,E$.

The effective $\alpha(t)$ for $\bar{p}p$ and pp differential cross sections are shown in fig. 9. The differences in the CCW and RRCP extrapolations are principally due to the different treatment of the helicity flip amplitudes. The large anti-shrinkage in the $\bar{p}p$ forward peak appears at momentum transfers greater than $0.3\ (\mathrm{GeV}/c)^2$ at energies of 10-50 GeV/c. This anti-shrinkage disap-

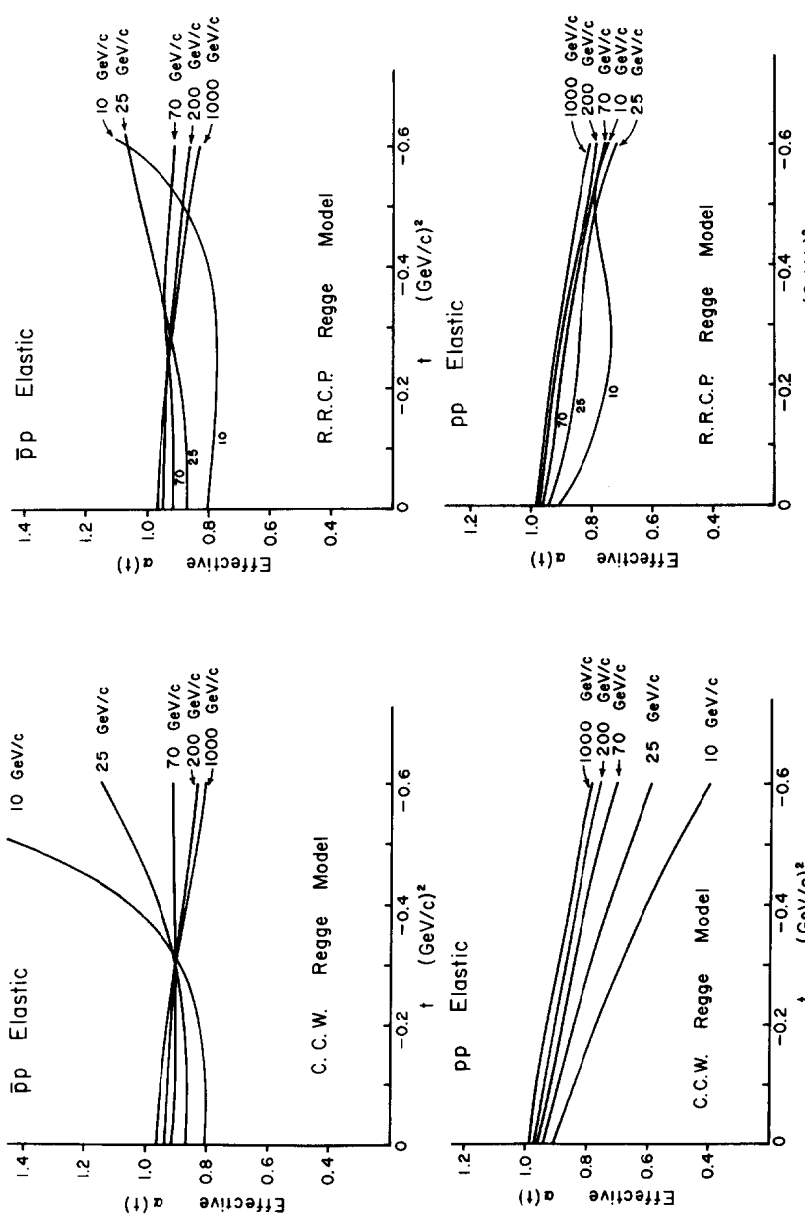

Fig. 9. Effective one-pole trajectory illustration of $\bar{p}p$ and pp elastic scattering projections of two Regge models (a) CCW (ref. [14]); (b) RRCP (ref. [15], solution 3).

$$2\alpha(t) - 2 = \frac{\ln[\frac{d\sigma}{dt}(E_2, t)/\frac{d\sigma}{dt}(E_1, t)]}{\ln[E_2/E_1]} .$$

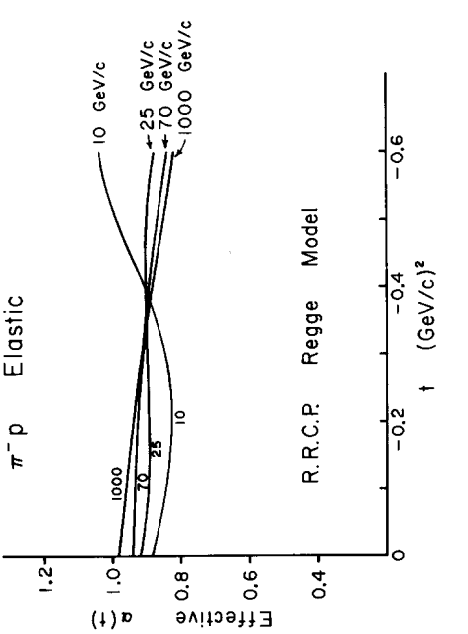

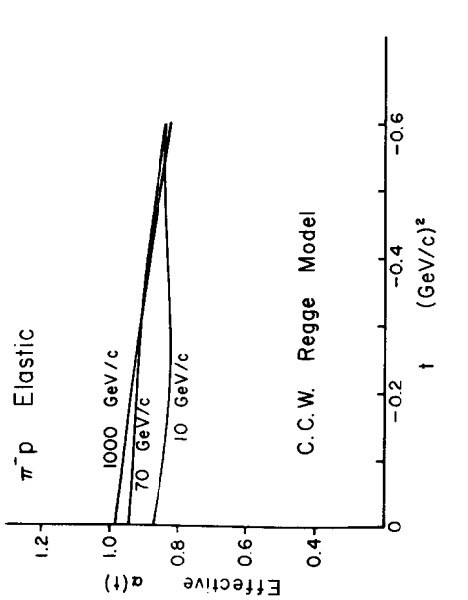

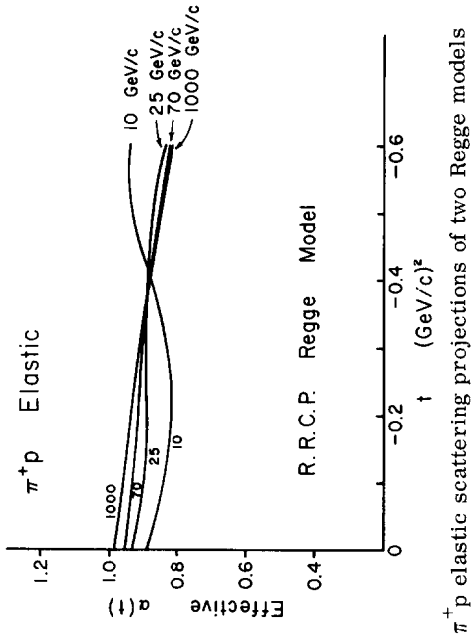

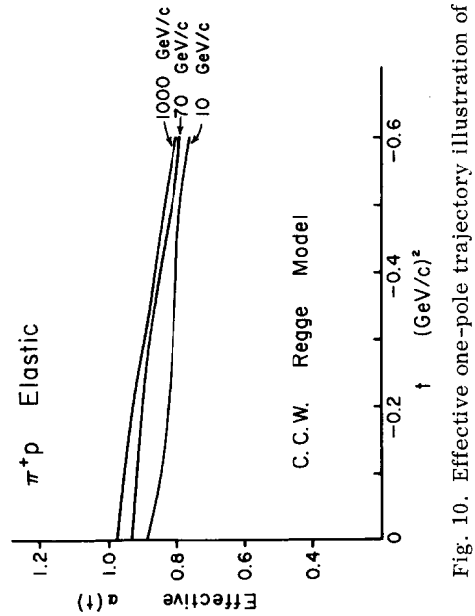

Fig. 10. Effective one-pole trajectory illustration of π^-p and π^+p elastic scattering projections of two Regge models (a) CCW (ref. [14]); (b) RRCP (ref. [15], solution 3).

pears around 70 GeV/c. In the pp forward peak the shrinkage gradually decreases with increasing energy until the Pomeranchuk limit is reached. By 200 GeV/c the shrinkage patterns of $\bar{p}p$ and pp look almost identical. Furthermore the shrinkage at 200 GeV/c has essentially reached the level expected from the Pomeranchuk slope. Fig. 10 shows the similar calculations of the effective $\alpha(t)$ for $\pi^{\pm}p$. No dramatic changes in the shrinkage pattern as a function of energy are observed.

All the above projections indicate that the cross sections will have essentially settled down to the Pomeranchuk contribution by 200 GeV/c. The contributions of the P' and ω trajectories are nearly damped out by this energy. Consequently, the measurement of shrinkage of the elastic scattering forward peaks at 200 GeV should determine if the Pomeranchuk exchange is in fact a moving pole in the j-plane. Conversely, if a fixed pole at $j=1$ or cuts in the angular momentum plane are the dominant singularities at high energy, then the direct experimental investigation of their properties will be possible.

The two Regge models considered above make essentially identical asymptotic predictions of the quantities $(d\sigma/dt)_{t=0}$, σ_{el} and $\sigma_{el}/\sigma_{total}$. These projections are shown in fig. 11. Once again it is evident that the Pomeranchuk limit is essentially reached by 200 GeV/c.

3.2. *Diffraction models*

Recently attempts have been made to interpret the pp elastic differential cross section data in terms of models that are more akin to the traditional diffraction formulations. The asymptotic projections of these models are dramatically different than those of the Regge models. The only quantitative fit to present data using a diffraction-like model has been presented by Krisch [2]. In this section we discuss the asymptotic projections of his model as representative of results to be expected from the customary diffraction models.

The pp elastic scattering data are parametrized in terms of a derived cross section $d\sigma^{\dagger}/dt$ which is assumed to be given by an incoherent sum of three Gaussians in the variable $\beta p_{\perp}$

$$\frac{d\sigma^{\dagger}}{dt} = \sum_{i=1}^{3} A_i \exp[-a_i \beta^2 p_{\perp}^2],$$

where β is the c.m. velocity and $p_{\perp}$ is the c.m. transverse momentum. The quantity $d\sigma^{\dagger}/dt$ is identical to $d\sigma/dt$ at small angle and is obtained from $d\sigma/dt$ at large angles through a particular prescription. This formula crudely describes the data over twelve orders of magnitude [2]. The variable $\beta^2 p_{\perp}^2$, which tends to $-t\{1+(t/s)\}$ at high energy, allows for shrinkage. The asymptotic shrinkage patterns predicted by the model are shown in fig. 12. By 200 GeV the shrinkage has essentially disappeared.

Unfortunately this fit does not account for an important aspect of the present pp data. As is generally the case with diffraction models the forward differential cross section is predicted to be constant with energy. From the Krisch fit the value

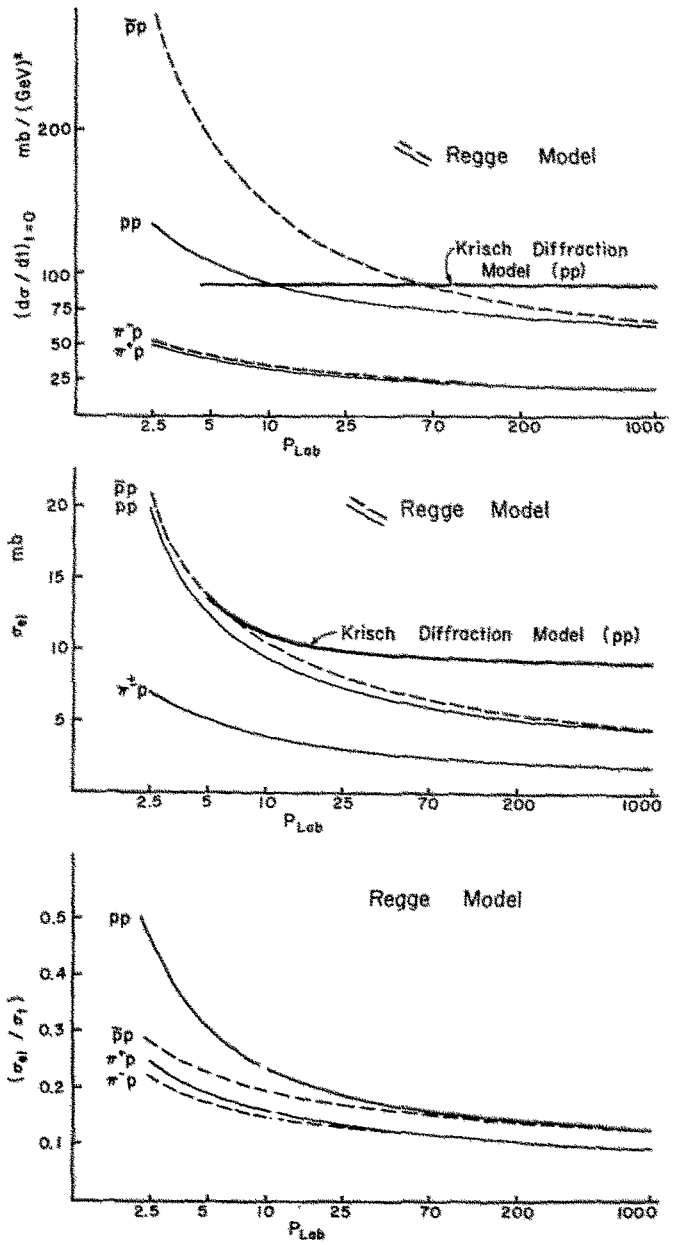

Fig. 11. Ultrahigh energy projections of (a) $(d\sigma/dt)_{t=0}$, (b) σ_{el}, (c) (σ_{el}/σ_t) from representative Regge models (refs. [14, 15]) for $\pi^{\pm}p$, pp, $\bar{p}p$ elastic scattering. Projections of the Krisch diffraction model (ref. [2]) are also shown.

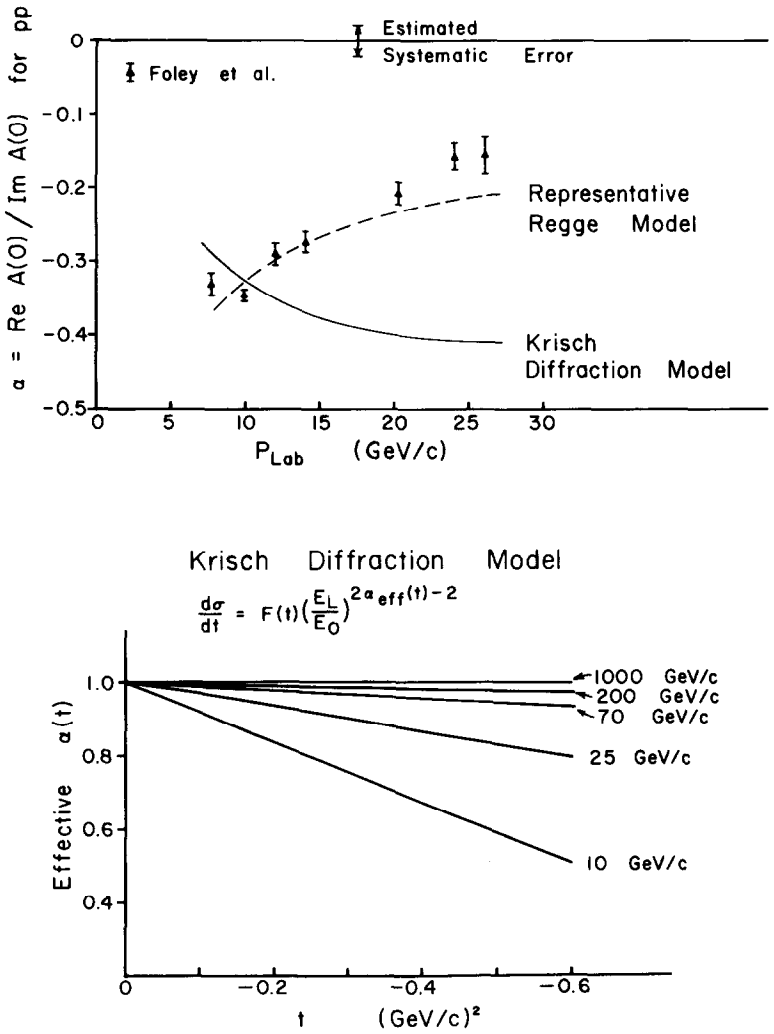

Fig. 12. Ratio of $\mathrm{Re}f(0)/\mathrm{Im}f(0)$ obtained from the Krisch model using the measured values of σ_t(pp) (ref. [1]) and assuming spin independence for forward pp scattering. The lower part of the figure shows an effective Regge trajectory for the Krisch model.

$$\left(\frac{\mathrm{d}\sigma}{\mathrm{d}t}\right)_{t=0} = 90\ \mathrm{mb/(GeV/}c)^2$$

is obtained (see fig. 11). Since the pp total cross sections decrease with increasing energy and

$$\left(\frac{\mathrm{d}\sigma}{\mathrm{d}t}\right)_{t=0} = \frac{\sigma_t^2}{16\pi}(1+\alpha^2),$$

where $\alpha = (\mathrm{Re}f/\mathrm{Im}f)_{t=0}$, we can deduce that the magnitude of α_{pp} would necessarily increase with energy in this model as illustrated in fig. 12. Barring spin dependence of the forward amplitude, which seems unnatural in a diffraction picture, this model is inconsistent with the measurements of α_{pp} (ref. [1]). Such difficulties are typical of attempts to use diffraction models to describe the $t = 0$ data over the present energy range where total cross sections are decreasing with energy. Thus any successful attempt to apply these types of diffraction models must be confined to a higher energy region than has been experimentally explored at present.

4. SUMMARY

Regge-pole models have provided a reasonably adequate description of total cross section and elastic-scattering data at present energies. Useful as such parametrization may be, there has been little in the way of critical experimental tests. In fact, because of the presence of the secondary trajectories which are important at present energies, it is likely that such critical tests must await completion of the new generation of accelerators. With this point in mind we have examined the features of present models in the ultrahigh-energy domain. Perhaps the most important result we have found is that the Pomeranchuk Regge pole amplitude completely dominates all the secondary trajectories above 200 GeV/c. Consequently, we can reasonably expect that experiments in the 200-400 GeV/c range will provide information bearing directly on the properties of this elusive amplitude. If Regge cuts play an increasingly important role at higher energies, then we might expect appreciable deviations from the Pomeranchuk Regge pole projections given here.

We anticipate that our extrapolations will be useful to physicists engaged in planning the early experiments to be carried out on the higher energy accelerators.

REFERENCES

[1] K. J. Foley et al., Phys. Rev. Letters 19 (1967) 193, 330, 857.
[2] A. D. Krisch, Phys. Rev. Letters 19 (1967) 1149.
[3] V. Barger and M. Olsson, Phys. Rev. 146 (1966) 1080.
[4] V. Barger and M. Olsson, Phys. Rev. Letters 18 (1967) 294.
[5] C. A. Levinson, N. S. Wall and H. J. Lipkin, Phys. Rev. Letters 17 (1966) 1122.
[6] V. Barger and L. Durand III, Phys. Rev. 156 (1967) 1525.
[7] V. Barger, M. Olsson and K. V. L. Sarma, Phys. Rev. 147 (1966) 1115; H. Sugawara and F. Von Hippel, Phys. Rev. 141 (1966) 1331.
[8] N. Cabbibo, L. Horwitz, J. J. J. Kokkedee and Y. Ne'eman, Nuovo Cimento 45A (1966) 275.
[9] B. Desai and P. Freund, Phys. Rev. Letters 16 (1966) 622; A. Ahmadzadeh, Phys. Rev. Letters 16 (1966) 952; Phys. Letters 22 (1966) 96; P. B. James and R. K. Logan, Phys. Letters 25B (1967) 38; S. Meshkov and G. B. Yodh, Phys. Rev. Letters 19 (1967) 603.
[10] W. Galbraith et al., Phys. Rev. 138 (1965) B913.

[11] G. Bellettini et al., Phys. Letters 19 (1965) 341.
[12] $\pi^- + p \rightarrow \pi^0 + n$ data (24 measurements):
P. Falk-Vairant et al., quoted in G. Höhler, J. Baacke and R. Strauss, Phys. Letters 21 (1966) 223;
I. Mannelli, A. Bigi, R. Carrara, M. Wahlig and L. Sodickson, Phys. Rev. Letters 14 (1965) 408;
A. V. Stirling et al., ibid. 14 (1965) 763.
$\pi^- + p \rightarrow n + \eta$ data (6 measurements):
O. Guisan et al., Phys. Letters 18 (1965) 200. We used 0.33 for the branching ratio $(\eta \rightarrow \gamma+\gamma)/(\eta \rightarrow \text{all})$.
$K^- + p \rightarrow \bar{K}^0 + n$ data (4 measurements):
P. Astbury et al., Phys. Letters 23 (1966) 396.
[13] Proc. CERN Topical Conf. on hadron collisions at high energy (1968), to be published.
[14] C. B. Chiu, S. Y. Chu and L. L. Wang, Phys. Rev. 161 (1967) 1563.
[15] W. Rarita, R. J. Riddell Jr, C. B. Chiu and R. J. N. Phillips, Phys. Rev. 165 (1968) 1615.